



Production and Characterization of Activated Carbon Derived from *Costus Afer* Leaves (*C. afer*) for the Adsorption of Methylene Blue Dye from an Aqueous Solution

King, L. J. ^{a*}, Obiukwu, O. O. ^a, Nwaji G. N. ^a,
Ekpechi D. A. ^a, Jerome, F. N. ^a and Ubani M. U. ^a

^a Department of Mechanical Engineering, Federal University of Technology, Owerri, Imo State, Nigeria.

Authors' contributions

This work was carried out in collaboration among all authors. All authors read and approved the final manuscript.

Article Information

DOI: <https://doi.org/10.56557/ajocr/2024/v9i28700>

Open Peer Review History:

This journal follows the Advanced Open Peer Review policy. Identity of the Reviewers, Editor(s) and additional Reviewers, peer review comments, different versions of the manuscript, comments of the editors, etc are available here: <https://prh.ikpress.org/review-history/12060>

Original Research Article

Received: 18/02/2024

Accepted: 21/04/2024

Published: 17/05/2024

ABSTRACT

In this work, *Costus afer* leaves (*C. afer*) was utilized as an agricultural waste material for the synthesis of activated carbon (AC) used for the adsorption of methylene blue dye from its aqueous solution. The raw material was prepared, chemically activated using KHCO_3 with an impregnation ratio of 1:3, and later carbonized at a temperature of 700°C in an inert N_2 atmosphere for 1 hour to produce activated carbon. The proximate analysis of the biomass revealed the percentage of ash content, moisture content, volatile matter, and fixed carbon present in the waste biomass. The raw

*Corresponding author: E-mail: kinglarry.20204249258@futo.edu.ng;

Cite as: King, L. J., Obiukwu, O. O., Nwaji G. N., Ekpechi D. A., Jerome, F. N., & Ubani M. U. (2024). Production and Characterization of Activated Carbon Derived from *Costus Afer* Leaves (*C. afer*) for the Adsorption of Methylene Blue Dye from an Aqueous Solution. *Asian Journal of Current Research*, 9(2), 232–250. <https://doi.org/10.56557/ajocr/2024/v9i28700>

and activated carbon produced were characterized using various tests such as: Scanning Electron Microscopy (SEM), Energy Dispersive X-Ray (EDX), Fourier Transform Infrared-(FTIR) Spectrometry, X-Ray Fluorescence (XRF), and Brunauer-Emmett-Teller (BET). The results revealed that the S_{BET} of the biomass increased from 400m²/g to 600m²/g after activation. Adsorption studies were carried out in batch mode to determine the influencing factors of adsorption with varying adsorbent dosage, contact time, and pH values. The adsorption experiment revealed high adsorption efficiency at an optimum parameter of dosage (0.2g), contact time (10 min), and pH (8) with a 70.58% removal of methylene blue dye. An increase in dosage, contact time, and pH above the optimum parameter leads to a decrease in percentage removal. The adsorption capacity was achieved using adsorption isotherm models like Langmuir and Freundlich. Adsorption of methylene blue validated the Langmuir model with an R^2 of 0.999 and a Q_m of 11.83 mg/g. These results show that activated carbon prepared from *Costus afer* leaves constitutes an effective low-cost material for the adsorption of Methylene dye from wastewater.

Keywords: Activated carbon; adsorption; costus afer leaves; isotherms; $KHCO_3$; methylene blue.

ABBREVIATIONS

AC : Activated Carbon
 CAL : Costus Afer Leaves
 $KHCO_3$: Potassium Bicarbonate
 ACCAL : Activated Costus Afer Leaves from $KHCO_3$
 MB : Methylene Blue
 ASTM : American Standard for Testing of materials
 BET : Brunauer Emmett and Teller
 EDX : Energy Dispersive X-ray
 FTIR : Fourier Transform infrared Spectroscopy
 SEM : Scanning Electron Microscopy
 XRF : X-ray Fluorescence

1. INTRODUCTION

One of the major global concerns is the discharge of toxic effluents into the environment, which poses hazardous threats to life and animals. These effluents contain dangerous contaminants like dyes, heavy metals, and organic compounds that are very harmful to lives when discharged without effective water treatment. Dyes are widely used in textiles, plastics, food, and photoelectrochemical industries. The removal of dyes from textile wastewater is crucial for mitigating environmental pollution by ensuring that wastewater complies with regulatory standards. According to research, Nigeria produces approximately 32 million tons of waste [1]. The textile, cosmetic, and clothing industries use dyes to color their products. The intensive use of organic dyes results in a high proportion of these compounds in wastewater, necessitating solutions for their removal and disposal. Dyes used in textile industries are acidic, basic, azo, and caustic dyes [2]. An

important basic dye is Methylene Blue (MB), which is widely used as a coloring agent for wool, cotton, and silk in the textile industry. Methylene blue is a commonly used cationic dye for coloring, which can also cause eye burns in humans and animals, dyspnea, and skin irritation [3]. In humans, extended contact with these dyes can lead to organ failure, diarrhea, heartburn, and tachycardia. These dyes are hazardous to the environment because of their toxicity, posing a major threat to aquatic ecology and living organisms because they are extremely poisonous and carcinogenic [4]. In addition, these dyes are non-biodegradable and harmful to humans when discharged into the environment because of their chemical structure. MB dye has some adverse effects on human health, but it also has potential applications in various fields. Thus, MB concentrations in water bodies have been rigorously controlled by environmental and health protection authorities, and these contaminants are given priority for elimination [5].

Today, innovative and modern water treatment solutions are being developed to manage the release of dangerous contaminants from wastewater. Several techniques such as coagulation, adsorption, solvent extraction, ion exchange, chemical precipitation, evaporation, and membrane filtration technologies have been employed in wastewater treatment at different time points [6-9]. Most of these methods are feasible in large-scale industries: but among these methods, adsorption has been an economically viable approach that can remove multiple contaminants simultaneously using a wide variety of low-cost adsorbents [10]. Adsorption is a waste treatment technique used in dye removal. A broad range of adsorbents remove common dyes from various sources.

Examples of these adsorbents include sawdust [11], fly ash [12], agricultural waste [13], graphene [14], and carbon nanotubes [15].

Activated carbon (AC) is widely used as a reliable adsorbent for the adsorption of color/dye from wastewater. AC is a carbonaceous material with an amorphous solid structure that has a high degree of porosity and a well-developed surface area with numerous oxygenated functional groups such as carboxylic acids, phenols, carbonyls, and lactones [16]. Owing to its unique properties, activated carbon, a porous carbonaceous material, has several applications in wastewater treatment, air purification, and desalination [17]. They are commonly prepared and produced from agricultural residues by carbonization and activation [18]. ACs are widely derived from agricultural wastes because of their low cost and economic abundance. These adsorbents can be defined as the substance on which the adsorbate is adsorbed. The adsorbate can be likened to the substance in the solution that is adsorbed by the adsorbent. Various adsorbents have been used in the production of AC from agricultural materials like peanut shells [19], coconut shells [20], cassava peeling [21], snail shells [22], and plantains [23]. Their high carbon content, low ash content, and high volatile matter make them suitable precursors for the production of AC [24].

Corn husk was investigated by Khodaie et al., [25] for the removal of methylene blue from wastewater using $ZnCl_2$ as an activating agent. The Langmuir isotherm model proved to be valid with an adsorption capacity of 298 mg/g. Groundnut shell chemically activated with H_2SO_4 was investigated by Melroy and Aravinda [26] for the removal of methylene blue from aqueous solution. The activated groundnut shell carbon results showed 95-99% of adsorption. Freundlich isotherm model was applied with an R^2 of 0.992. Oil palm wastes were investigated by Baloo et al., [27] for the adsorptive removal of methylene blue dye from an aqueous solution. The isotherm model was better represented by the Langmuir model with an R^2 of 0.979. Bush cane bark powder was investigated by Enenebeaku et al., [28] for the adsorption of methylene blue from an aqueous solution. The adsorption isotherm obeyed the Freundlich isotherm model with an R^2 of 0.9579 and an adsorption capacity of 23.49 mg/g.

Costus afer (*C. afer*) is a plant commonly known as ginger lily, spiral ginger, or bush cane. Various

online searches have revealed that the plant has been used for traditional and medicinal purposes to treat diabetes, arthritis, stomach aches, and skin diseases [29]. It is abundant in the East region of Nigeria and is used for the aforementioned purposes. In Nigeria, it is known as Okpete in the Igbo language, mbitem in the Efik language, kakii-zuwa in the Hausa language, and tete-egun in the Yoruba language [30-32]. The utilization of *C. afer* as a precursor for the production of activated carbon remains scarce in literature but yields great potential for this course. Therefore, this study aimed to prepare and produce activated carbon from CAL using $KHCO_3$ as an activating agent for the adsorption of methylene blue dye from its aqueous solution. The physical and chemical properties of ACCAL were determined using different characterization techniques: and the effects of influencing parameters such as adsorbent dosage, contact time, and pH were studied. The process reported here is important for the conversion of waste into wealth.

2. MATERIALS AND METHODS

2.1 Apparatus and Equipment List

The following apparatus and equipment were used in this work: Gallenamp Tube Furnace – Carbolite, Vertical Reactor, Dry Oven, Jaw Crusher (RetschBB2), Planetary Ball Mill (OVERUFLD S/No: 810), pH Meter-Hannah Pocket-sized pH Meter, Surface Area Analyzer (TC03), UV-Spectrophotometer, Analytical Balance (DRAWELL), Weighing Balance (OHAUS DV215CD), Scanning Electron Microscopy (SEM) (Phenom Prox), Fourier Transform Infra-Red Spectroscopy (FTIR) (Agilent Technologies, Cary 630 FTIR, Happ-Genzel, 4000-650 cm^{-1}), Plastic brush, Crucibles, Magnetic stirrer, Analytical. Hot Plate/Stirrer, Volumetric Flask, Funnel, Measuring flask, Spatula, Dropper.

2.2 Raw Materials Collection

Costus afer leaves (*C. afer*) were used as precursors because of their physical properties and abundance at the Federal University of Technology, Owerri's School region. These leaves were collected from bushes around Umuchima and transported to the laboratory. The leaves were washed carefully to remove dirt particles and impurities from their surfaces. After washing, the leaves were sun-dried for 3-4 days to eliminate moisture content and dried in an

oven for 4 hours at a temperature of 120°C. The leaves were crushed using a blender. Furthermore, the samples were sieved using a laboratory sieve to obtain very fine particles. The samples were placed in a safe place and labeled (Raw CAL) for further analysis.

2.3 Chemical Activation of CAL with KHCO_3

The chemicals used in this study for activation purposes were of analytical grade. The method applied in the chemical activation of CAL coincided with recent research by Liu et al., [33] with slight modifications. In a crucible, 4g of the dried raw sample was weighed using a weighing balance and mixed in 10g of KHCO_3 using an impregnation

ratio of 1:3. The mixture was ground for 30 min to obtain a fine mixture, after which it was poured into a reactor, placed in a tube furnace, and heated to 700°C in an N_2 atmosphere in the absence of air for 1 h. As dark porous structures developed, the carbonized samples were allowed to cool to room temperature. To ensure that all contaminants and traces of leftover salts were removed from the activated samples and that the final products had a pH of 7 (neutral), they were thoroughly cleaned using distilled water (DI). Finally, the activated samples ($\text{ACCAL}_{\text{KHCO}_3}$) after washing were dried in an oven at 150°C for 3 h [34]. The activated samples were allowed to cool and stored in an airtight container labeled ACCAL-KHCO_3 . Fig. 2. shows a schematic of the *Costus afer* activated carbon preparation.



Fig. 1. *Costus afer* leaves found in umuchima environs

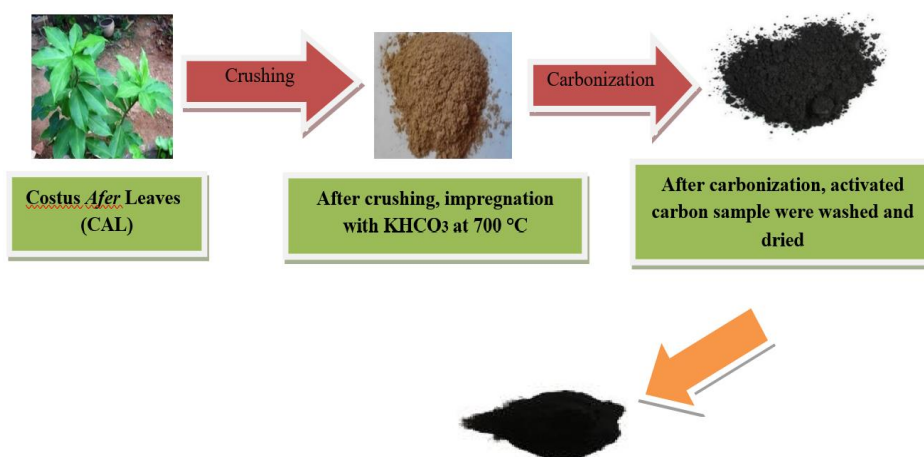


Fig. 2. Schematic diagram of *costus afer* AC preparation

2.4 Methylene Blue Dye Solution

The chemicals used to prepare the MB solution were of high analytical grade. Methylene Blue dye was purchased from the Zaria Chemical Laboratory, Nigeria. A stock solution of methylene blue dye was prepared by dissolving 0.5g of commercially available methylene blue in 1 L of distilled water to obtain a stock concentration of 50 mg/L. Experimental dye solutions of desired concentrations were prepared by appropriate dilution of the stock solution.

2.5 Proximate Analysis

When samples were heated and handled under specified circumstances, a set of tests known as proximate analysis was used to determine the composition of the accessible macronutrients (Ash content, moisture content, volatile matter, and fixed carbon content) for raw *costus afer* leaves. The ash content, moisture content, volatile matter and fixed carbon of the material samples was determined via the American Society for Testing and Materials standard method [35-37].

2.5.1 Ash content

2.0 g of dry raw sample was weighed inside a crucible, oven-dried at 105°C, and later introduced into a tube furnace (Gallenhamp) that was then heated to 600°C at a heating rate of 10°C min⁻¹ for 1 hr. The sample was further cooled and weighed in a weighing balance.

$$\text{Ash content (\%)} = \frac{W_1 - W_2}{W_3} \times 100 \quad (1)$$

Where W1 = Weight of Crucible + Sample (g), W2 = Weight of Crucible + Sample after (g), and W3 = Weight of Sample (g).

2.5.2 Moisture content

A 2.0 g dried raw sample in a cleaned crucible was oven-dried at 110°C for 3 h until the weight of the samples remained constant. Samples were dried, cooled in a desiccator at room temperature, and then weighed again to calculate the moisture content using the following formula:

$$\text{Moisture Content (\%)} = \frac{W_1 - W_2}{W_1} \times 100 \quad (2)$$

Where, W1 = initial weight of sample in grams, W2 = final weight of the sample (in grams) after drying.

2.5.3 Volatile matter

A dry sample (1.0 g) was weighed inside a crucible, oven-dried at 105°C, and heated to 600°C for 1 h in a tube furnace (Gallenhamp) at a heating rate of 10°C min⁻¹. The carbonized sample was then allowed to cool to ambient temperature, removed from the furnace, and stored in a desiccator.

2.5.4 Fixed carbon

The Fixed carbon content was obtained by subtracting the percentage of moisture, ash, and volatile matter content of the materials from a hundred percent according to the method of Alongamo et al., [31]:

$$\text{Fixed carbon (\%)} = 100 - \text{moisture(\%)} - \text{ash content (\%)} - \text{volatile matter(\%)} \quad (3)$$

2.6 Characterization of Adsorbents

The surface morphology of the adsorbent was analyzed using a scanning electron microscope ((Phenom-World) operated at a voltage of 15 kV. Scanning electron microscopy was used to study the morphology and surface structure of the adsorbent material [38]. SEM images of the raw and activated samples revealed the structure and morphology of the samples. Before scanning the adsorbent, the samples were sputtered on carbon tape and set on a fixed reduction sample holder, and SEM images were obtained. SEM analysis was performed using an energy-dispersive X-ray (EDX) spectrometer to reveal the elemental composition of the samples. BET analysis was used to determine the specific surface area of the raw and activated CAL. The raw and activated samples were degasified to remove gases and impurities. These samples were pretreated in a flow of pure nitrogen gas at 30 ml/min for 1 h at 250°C before surface area measurements [39]. XRF analysis was used to determine the elemental composition of the materials found in the adsorbent [20]. The functional groups of the samples were examined using FTIR Spectroscopy. FTIR spectroscopy was performed using Agilent Technologies (Cary 680 FTIR) [40].

2.7 Batch Adsorption Experiment

Batch adsorption studies were performed at different dosages, contact times, and pH values to evaluate the adsorption parameters of ACCAL_{KHCO₃} for the removal of Methylene blue from its aqueous solution. The batch adsorption experiments were performed in a set of 100 ml conical flasks with varying amounts of adsorbent dosage, contact time, and pH. The percentage of methylene blue removal was calculated as follows:

$$\% RE = \frac{C_o - C_i}{C_o} \times 100 \quad (4)$$

Where RE (%) is the MB removal percentage, C_o is the initial MB concentration (mg/L) in the wastewater, C_i is the MB concentration at time t , (mg/L) [41].

The amount of MB adsorbed per unit mass of on the adsorbents, q_e , was determined using the equation (3.5) below:

$$q_e = \frac{C_o - C_e}{m} \times V \quad (5)$$

Where q (mg/g) is the adsorption capacity, V (L) is the volume of MB solution, C_o (mg/L) and C_e (mg/L) are the initial and equilibrium concentrations of methylene blue, and m (g) is the weight of the adsorbents (g) [42].

2.8 Adsorption Isotherm

Adsorption isotherm models are vital for providing the mechanism of the adsorption process, which is pertinent for the design of the adsorption process. Adsorption isotherms are crucial for comprehending catalytic processes and the adsorption mechanism [43]. They are also employed to optimize the adsorbent mass during the adsorption process and to model experimental equilibrium data [44]. In this study, Langmuir and Freundlich models that express experimental isotherm data were used. The Langmuir isotherm is based on the equilibrium between adsorption kinetics and was originally proposed by Langmuir [45]. The adsorption isotherm is crucial in the determination and optimization of the adsorption system. Scientifically, the adsorption isotherm is a functional expression for the variation of adsorption with the concentration of the adsorbate in the bulk solution. The Langmuir isotherm model is based on the assumption of

ideal adsorption in which uptake occurs on the adsorbent surface by monolayer adsorption.

Almasi [46] described the adsorption isotherm as the relationship between the mass of adsorbed dye per unit mass of adsorbent. The linear form of Langmuir isotherms is expressed in given as:

$$\frac{C_e}{Q_e} = \frac{1}{KLQ_m} + \frac{C_e}{Q_m} \quad (6)$$

Where C_e is the equilibrium concentration (mg/L), Q_e is the amount adsorbed at equilibrium (mg/g), Q_m (mg/g) is the maximum adsorption capacity, and KL (L/mg) is the Langmuir constant. The values of Q_{max} and KL were calculated from the intercept and slope of the linear plot of C_e/q_e against C_e using Origin Pro 9.

The Freundlich isotherm was the first adsorption equilibrium equation proposed in the literature (Freundlich [47]). Freundlich isotherm revealed the interaction of dye adsorption on the heterogeneous surface. Freundlich linear equation is expressed as follows:

$$\ln Q_e = \ln K_f + \frac{1}{n} \ln C_e \quad (7)$$

Where C_e is the equilibrium concentration (mg/L), Q_e is the amount adsorbed at equilibrium (mg/g), and K_f and n are Freundlich constants.

3. RESULTS AND DISCUSSION

3.1 Proximate Analysis

The results of the proximate analysis for the determination of macronutrients of *costus afer* leaves are shown in Fig. 3., which reveals, 1.5% ash content, 36.6% moisture content, 29.2% volatile mate, and 36.7% fixed carbon. From the results obtained, CAL exhibited characteristics of a good precursor for the production of activated carbon. Fig 3. and Table 1. show that the raw CAL contains a good percentage of carbon which is an essential factor for the selection of a precursor with high adsorptive potentials for the production of activated carbon [48]. These findings were compared to other works of literature in terms of the proximate analysis as tabulated in Table 1.

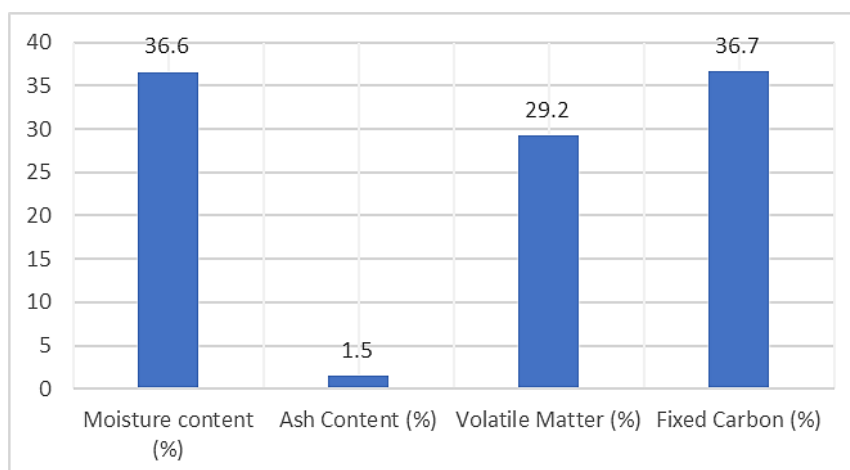


Fig. 3. The proximate analysis of Costus afer leaves

Table 1. The proximate composition of various adsorbents

Raw Adsorbent	Proximate Analysis (%)				References
	Ash Content	Volatile Matter	Moisture Content	Fixed Carbon	
Cassava Peeling	8.0	13.0	1.0	78	Alongamo et al., [21]
Rumex abyssinicus plant	9.82	18.74	2.95	68.94	Fito et al., [49]
Coconut Shell	7.78	63.76	12.86	15.58	Khuluk et al., [50]
Coconut Husk	5.3	41.2	14.2	39.3	Asadu et al., [20]
Pure Lignin	11.6	36.6	7.9	43.9	Bedmohata et al., [39]
Costus afer	1.5	29.2	36.6	36.7	This work

Table 2. BET-surface area of different adsorbents

Adsorbents	Activating Agent	BET-Surface Area (m ² /g)	References
Groundnut shell	KOH	691.69	Kumari et al., [52]
Spathodea campanulata	H ₃ PO ₄	1054	Dimbo et al., [51]
Rice husks	H ₃ PO ₄	244.479	Sawasdee et al., [53]
Costus afer leaves	KHCO ₃	600	(This work)

3.2 Specific Surface Area

AC produced from CAL (600 m²/g) using KHCO₃ as an activating agent is higher than that of raw CAL (400 m²/g). Activated carbon with a higher surface area and a well-developed pore structure provides more sites for adsorption, leading to increased adsorption capacity [51]. Table 2 compares the specific surface areas of different activated adsorbents with the findings of this work. The increased surface area indicates that the adsorbent has more active sites on its surface, which may improve the large-scale industrial adsorption of contaminants from textile effluent. Therefore, the result of the BET-surface

area proves that ACCAL_{KHCO₃} can be commercially applicable for industrial water purification.

3.3 Characterization of Adsorbent

3.3.1 Fourier-transform infrared spectroscopy (FTIR)

The location of the wavenumber (cm⁻¹) in the range 650 to 4000 cm⁻¹ obtained from the results of the Fourier-Transform Infrared (FTIR) spectra for the raw and activated samples is shown in Fig. 4, and their major bands are tabulated in Table 3 From the results obtained from the

spectral analysis of raw CAL, a broad absorption band centered around 3000-3500 cm^{-1} , was observed at 3261.4 cm^{-1} corresponding to O-H bond stretching characteristic of carboxylic acids, alcohol, or water. The pattern observed in this study is somewhat comparable to that of previous research on the production of activated carbon [54-55]. The raw samples showed peaks between 2800 – 3000 cm^{-1} , with maximum peaks at 2922.2 cm^{-1} and 2851.4 cm^{-1} for raw CAL, which indicates the presence of C-H (CH₃ and CH₂) stretch of the aliphatic hydrocarbon [56]. It is noticed that this broadband decreases after carbonization and leads to the absence of water molecules on the surface of the material. The disappearance of these peaks is visible after carbonization because of the loss of the hydroxyl group and absorbed water [57]. Bands around 2150 cm^{-1} - 2250 cm^{-1} correspond to the presence of C≡C Stretching. These peaks were located in the activated samples at 2109.7 cm^{-1} for ACCAL_{KHCO₃}. Sharp peaks were observed in the activated CAL sample spectra at 1990.4 cm^{-1} indicating cyanide and thiocyanide ion stretches. Broad peaks of the raw CAL at 1636.3 cm^{-1} are due to the conjugated C=C stretching vibration, which reveals the presence of aromatic carbon-carbon double bonds. It can be observed that the raw samples had more peaks than the activated ones, which implies that they have more functional groups. This agrees with the literature that carbonization and activation could lead to the disappearance of some functional groups [40].

3.3.2 Scanning electron microscopy (SEM) of raw and activated CAL

Scanning electron micrographs of raw and activated CAL are presented in Figs. 5(a), 5(b), 5(c) and 5(d). From the SEM images at low and high magnifications, it can be noticed that the surface morphology of the raw CAL has fine and well-arranged structures. It also contains a smooth and well-packed microstructure with

fistulous crystallites, which indicate minerals. These glowing crystallites indicate calcium, aluminum, and iron. The SEM micrograph of the activated CAL in Figs. 5(c-d) reveals that the sample is highly porous. The pore structure of the activated CAL is more developed than that of the raw CAL, which is consistent with previous studies showing that activation increases the pore structure of a material [58]. From the images of the activated CAL, as shown in Fig. 5(c-d), the activated samples have increased their porous network, which in turn increases their surface area, making them suitable for adsorption.

3.3.3 Energy dispersive X-ray spectroscopy (EDX) of raw and activated CAL

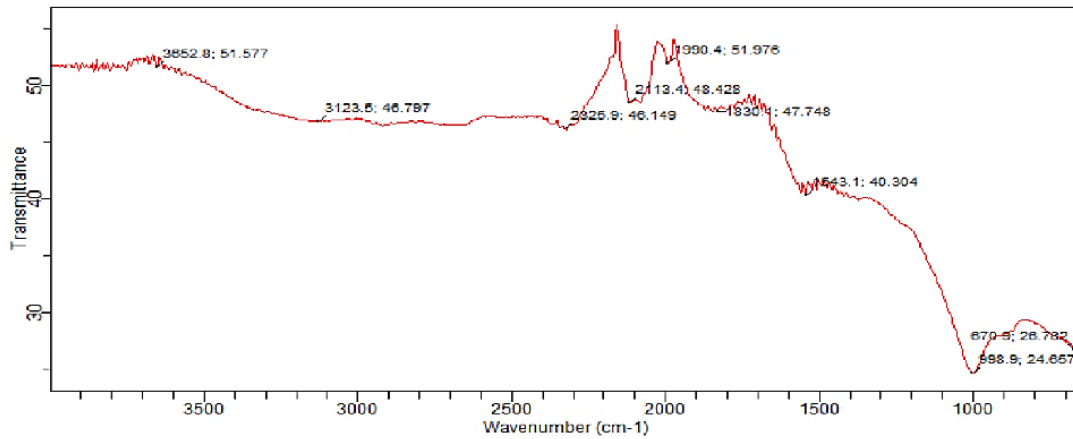
EDX spectral analysis was used to probe the elemental composition of the raw and activated samples. The energy dispersive X-ray Spectroscopy (EDX) spectral results for *Costus afer* (CAL) leaves are presented in Tables. 4 and 5 EDX analysis generated data comprising spectra with peaks corresponding to various components, as shown in Figs. 6(a) and 6(b). EDX spectra taken at 15 Kv, FOV: 537 μm , and a BSD full detector.

3.3.4 X-ray fluorescence (XRF) analysis of raw CAL

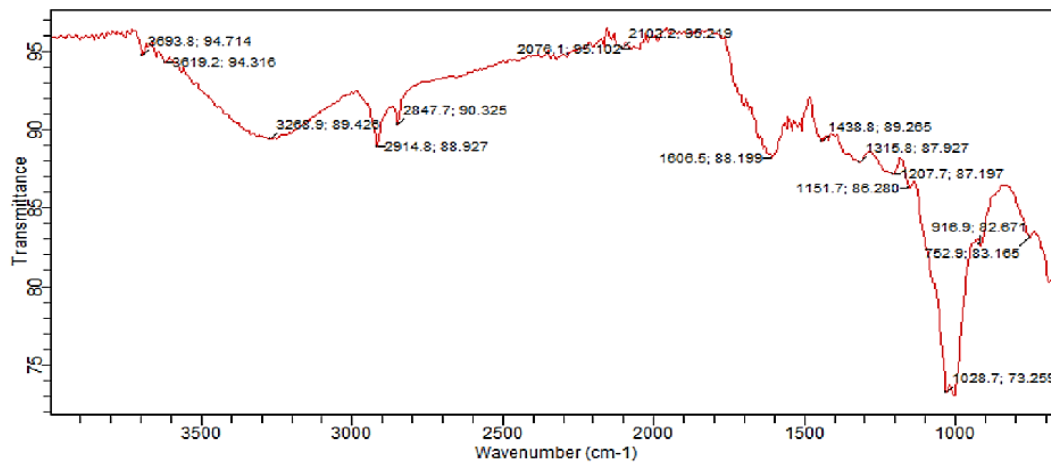
X-ray Fluorescence (XRF) analysis for the raw CAL was performed as shown in Fig. 7, confirming that the sample consisted of a good amount of carbon. XRF analysis was performed on the raw sample (CAL) to determine the chemical compounds and concentrations present in the sample. Fig. 7 reveals the dominant compounds and their concentrations in CAL, namely, potassium oxide (51.383%), calcium oxide (23.695%), alumina (5.915%), and silica oxide (4.659%), while other components were found in nominal amounts.

Table 3. Characteristics bands in the FTIR spectra of raw and activated biomass

S/No	Wavenumber/Frequency (Cm^{-1}) of Absorption band
1	3261.4
2	2922.2, 2851.4
3	2109.7
4	1636.3
5	3852.8, 3693.8, 2325.9, 2076.1, 1207.7, 1028.7, etc.



(a)



(b)

Fig. 4. FTIR Spectra of: (a) Raw CAL (b) Activated CAL

Table 4. EDX spectrum of CAL

Element Number	Element Symbol	Element Name	Atomic Conc.	Weight Conc.
6	C	Carbon	76.47	66.43
7	N	Nitrogen	16.94	17.16
19	K	Potassium	3.00	8.50
15	P	Phosphorus	0.69	1.54
12	Mg	Magnesium	0.72	1.27
20	Ca	Calcium	0.43	1.24
14	Si	Silicon	0.53	1.08
17	Cl	Chlorine	0.24	0.63
16	S	Sulfur	0.26	0.59
13	Al	Aluminium	0.27	0.53
11	Na	Sodium	0.30	0.50
26	Fe	Iron	0.08	0.34
22	Ti	Titanium	0.06	0.20
Total				100

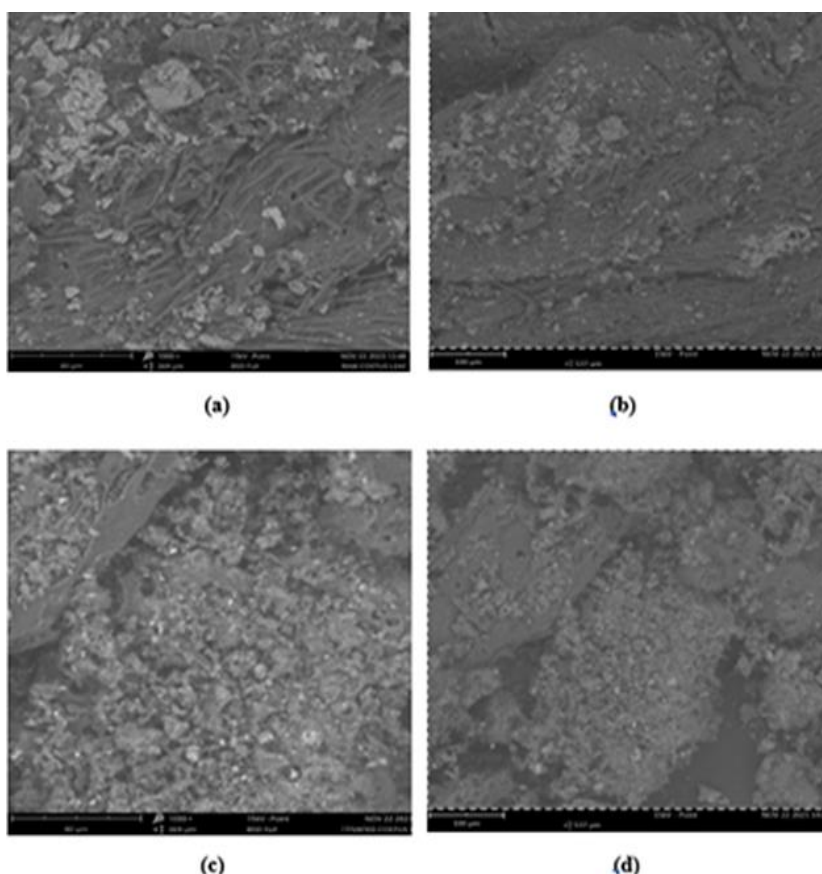


Fig. 5. SEM Images of (a) CAL at low magnification (b) CAL at high magnification (c) ACCAL_{KHCO3} at low magnification (d) ACCAL_{KHCO3} at high magnification

Table 5. EDX spectrum of activated CAL (ACCAL_{KHCO3})

Element Number	Element Symbol	Element Name	Atomic Conc.	Weight Conc.
6	C	Carbon	87.88	79.38
7	N	Nitrogen	6.85	7.22
20	Ca	Calcium	1.14	3.42
14	Si	Silicon	0.95	2.02
26	Fe	Iron	0.48	2.00
15	P	Phosphorus	0.77	1.80
12	Mg	Magnesium	0.75	1.38
19	K	Potassium	0.35	1.03
13	Al	Aluminium	0.29	0.59
11	Na	Sodium	0.26	0.45
16	S	Sulfur	0.16	0.39
17	Cl	Chlorine	0.09	0.25
22	Ti	Titanium	0.02	0.09
Total				100

3.4 Adsorption Experiment Parameters

3.4.1 Effect of adsorbent dosage

The effect of the adsorbent dosage of activated carbon on the percentage removal of MB is

shown in Fig. 8. The adsorbent dosage was varied from 0.1g to 0.5g for 10ml of 50mg/L solution at a constant time of 10 min and pH of 7. As observed from the graph in Fig. 8. An increase in the dosage increases the percentage removal of MB. The optimum dose of ACCAL is

0.2g with a percentage removal rate of 70%. After the optimum dose is reached, the percentage removal efficiency declines thereafter. These may result from active sites induced by agglomeration and particle clustering. Clustering reduces the number of adsorption sites accessible to an adsorbate from the solution [59].

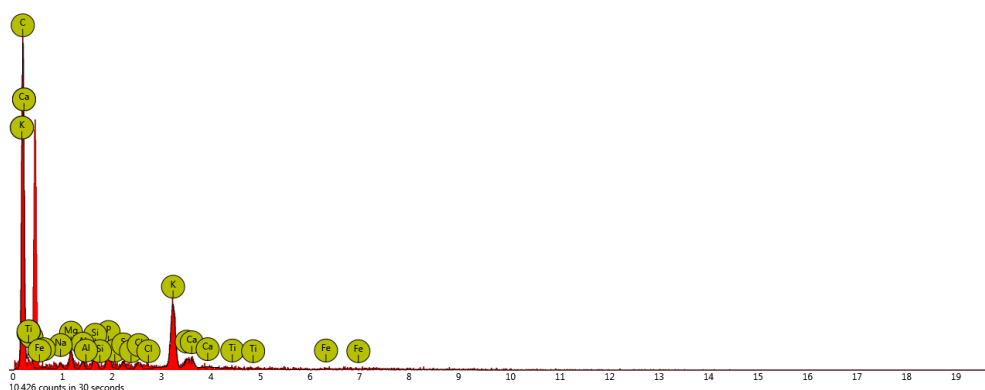
3.4.2 Effect of contact time

The effect of contact time is a vital factor in the percentage removal of MBD from its aqueous solution. For this experiment, an adsorbent dosage of 0.2g and a pH of 7 were kept constant while the time was varied from 5 min to 25 min at a constant MB solution of 10 ml of 50 mg/L. From Fig. 9, it can be seen that an increase in contact time leads to an increase in the removal of MB from its aqueous solution. The optimum time was 10 min, and thereafter, a reduction in the percentage removal rate of MB was observed. The highest percentage of removal (69.9%) was recorded at 10 min. Beyond the optimum time, a

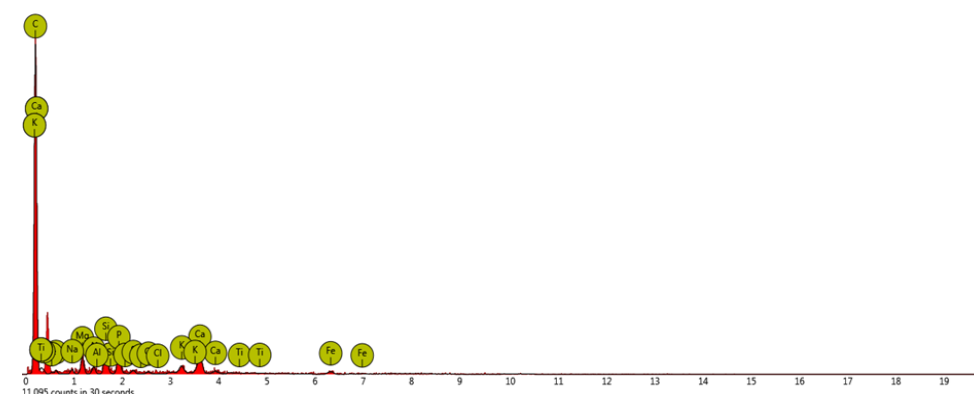
gradual decrease in the percentage removal was observed, which may be due to the lack of active sites or dislodged MB molecules [60-62].

3.4.3 Effect of pH

Fig. 10 shows the effect of pH on the percentage removal of methylene blue dye at a constant time of 10 min, constant solution of 10 ml of 50 mg/L, and constant adsorbent dosage of 0.2g. The effects of initial pH on the percentage removal of MB dye solution at a concentration of 100 mg/L were studied by varying the pH from 2 to 10. As the pH increases, it tends to increase the percentage of methylene blue removal. The percentage removal of the methylene blue dye from its aqueous solution by ACCAL_{KHCO3} was optimum at pH 8, with a percentage removal rate of 66.5%. As shown in Fig. 10, at pH 2–4, there was a slightly constant rate of percentage removal of MB and a steady increase from pH 4 to 6. Above the optimum pH of 8, there was a gradual decrease in the percentage removal of the MB dye [63].



(a)



(b)

Fig. 6. EDX spectrum of (a) CAL (b) ACCAL_{KHCO3}

CrossRoads Scientific XRS-FP Analysis Report

File: C:\Users\Xenemetrix\3D Objects\New folder (49)\RAW COSTUS.str

1:55:52 AM 14-Nov-23

Comment line

#	Thick	Type	Error	Units	Density	Norm.	Total
1	0.00	Bulk	0.00	mg/cm2	0.00F	On	100.00

Layer	Component	Type	Concn.	Error	Units	Mole%	Error
1	SiO2	Calc	4.659	0.601	wt. %	5.994	0.773
1	V2O5	Calc	0.000	0.000	wt. %	0.000	0.000
1	Cr2O3	Calc	0.038	0.037	wt. %	0.020	0.019
1	MnO	Calc	0.087	0.030	wt. %	0.095	0.033
1	Fe2O3	Calc	1.134	0.049	wt. %	0.549	0.024
1	Co3O4	Calc	0.022	0.026	wt. %	0.007	0.008
1	NiO	Calc	0.011	0.021	wt. %	0.012	0.022
1	CuO	Calc	0.227	0.022	wt. %	0.220	0.022
1	Nb2O3	Calc	0.029	0.018	wt. %	0.010	0.006
1	WO3	Calc	0.011	0.084	wt. %	0.004	0.028
1	P2O5	Calc	1.847	0.258	wt. %	1.006	0.140
1	SO3	Calc	4.048	0.249	wt. %	3.908	0.241
1	CaO	Calc	23.695	0.487	wt. %	32.662	0.671
1	MgO	Calc	0.000	0.000	wt. %	0.000	0.000
1	K2O	Calc	51.383	0.501	wt. %	42.166	0.411
1	BaO	Calc	0.000	0.000	wt. %	0.000	0.000
1	Al2O3	Calc	5.915	1.915	wt. %	4.484	1.452
1	Ta2O5	Calc	0.000	0.000	wt. %	0.000	0.000
1	TiO2	Calc	0.202	0.067	wt. %	0.195	0.065
1	ZnO	Calc	0.146	0.019	wt. %	0.138	0.019
1	Ag2O	Calc	0.030	0.092	wt. %	0.010	0.031
1	Cl	Calc	3.105	0.119	wt. %	6.770	0.259
1	ZrO2	Calc	0.009	0.017	wt. %	0.006	0.011
1	SnO2	Calc	3.401	1.563	wt. %	1.744	0.802

Elmt	Line	Cond	Ratio	Intensity	Error	Intensity	Conc.	Conc	Calibration
	Code		Method	(c/s)	(c/s)	Method		Method	Coefficient
O	Ka	0	None	0.000	0.0000	Gaussian	25.491	None	0.000
Mg	Ka	1	None	0.000	1.7146	Gaussian	0.000	FP	0.000
Al	Ka	1	None	10.382	3.3610	Gaussian	3.130	FP	0.000
Si	Ka	1	None	41.283	5.3270	Gaussian	2.178	FP	0.000
P	Ka	1	None	52.420	7.3146	Gaussian	0.806	FP	0.000
S	Ka	1	None	197.775	12.1785	Gaussian	1.621	FP	0.000
Cl	Ka	1	None	457.799	17.5180	Gaussian	3.105	FP	0.000
K	Ka	1	None	6335.759	61.8313	Gaussian	42.656	FP	0.000
Ca	Ka	1	None	1609.793	33.0865	Gaussian	16.935	FP	0.000
Ti	Ka	1	None	20.153	6.7328	Gaussian	0.121	FP	0.000
V	Ka	1	None	0.000	6.6603	Gaussian	0.000	FP	0.000
Cr	Ka	1	None	7.815	7.5857	Gaussian	0.026	FP	0.000
Mn	Ka	1	None	25.561	8.8211	Gaussian	0.067	FP	0.000
Fe	Ka	1	None	364.353	15.7832	Gaussian	0.793	FP	0.000
Co	Ka	1	None	8.872	10.4477	Gaussian	0.016	FP	0.000
Ni	Ka	1	None	5.619	10.2559	Gaussian	0.009	FP	0.000
Cu	Ka	1	None	129.776	12.7983	Gaussian	0.181	FP	0.000
Zn	Ka	1	None	93.157	12.4760	Gaussian	0.117	FP	0.000
Zr	Ka	1	None	4.792	8.7062	Gaussian	0.007	FP	0.000
Nb	Ka	1	None	14.009	8.5078	Gaussian	0.023	FP	0.000
Ag	Ka	1	None	1.603	4.9255	Gaussian	0.028	FP	0.000

Fig. 7. XRF of raw CAL

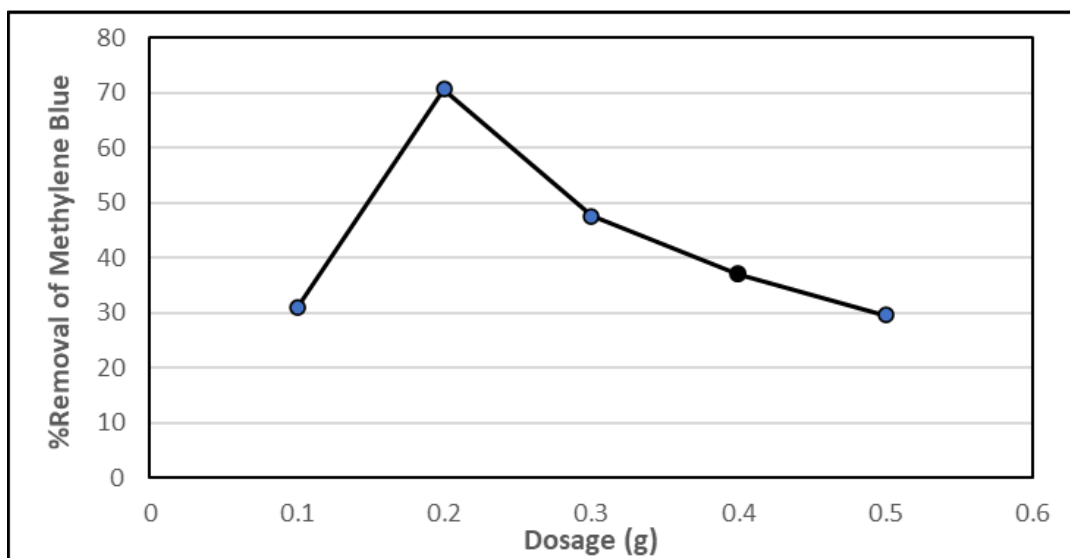


Fig. 8. Effect of adsorbent dose on the percentage removal of MB

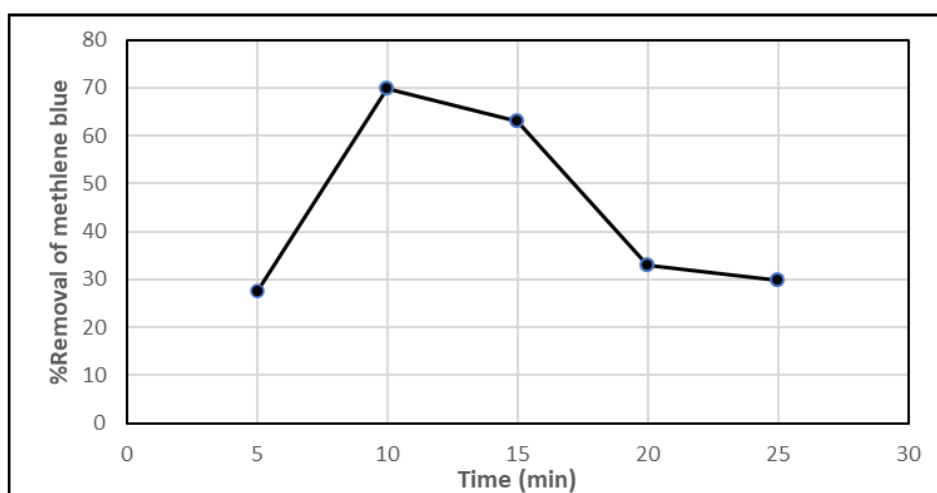


Fig. 9. Effect of contact time on the percentage removal of MB

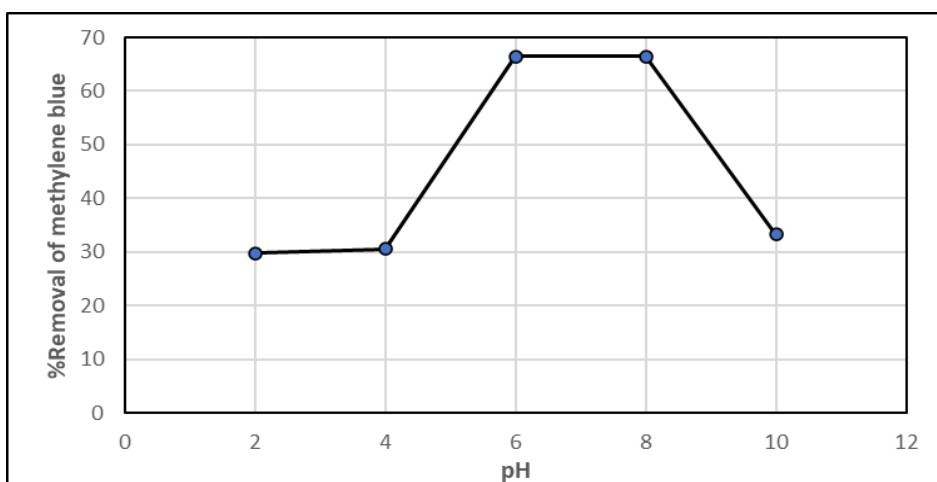


Fig. 10. Effect of pH on the percentage removal of MB

3.5 Adsorption Isotherm

Figs.11 and 12 show the Langmuir and Freundlich isotherm plots. For the Langmuir and Freundlich isotherm models, the coefficients (R^2) were 0.999 and 0.9519, respectively. The data fit well with the Langmuir isotherm. Langmuir and Freundlich plots for MB adsorption were analyzed for adherence using linear regression. The adsorption was found to be accurately characterized by the Langmuir and Freundlich adsorption isotherm models, with validity from the Langmuir isotherm model, which showed a greater R^2 of 0.999. The values of Q_m , RL , and KL were calculated from the slope and intercept of the plot and are presented in Table 6. RL is the separation factor that determines whether the adsorption process is favorable, unfavorable, or irreversible. If the value of RL is <0 , it indicates

an unfavorable adsorption process; RL between 0 and 1 ($0 = RL < 1$), shows a favorable adsorption, while $RL > 1$ shows an irreversible adsorption type. According to Malik [64], a value of $1/n < 1$, indicates the presence of new adsorption sites that will lead to an increase in adsorption capacity. In addition, $1/n > 1$ indicates weakness in the adsorption bond and a decrease in the adsorption capacity. Conversely, the Langmuir isothermal feasibility (RL) and Freundlich isotherm constant associated with intensity ($1/n$) were 0.6163 and 0.5117, respectively, indicating a favorable adsorption process. Similar methods have also been used by other researchers to perform adsorption isotherms [44, [65-66]. The capacity of $ACCAL_{KHCO_3}$ was found to be 11.83 mg/g in the Langmuir model for the removal of methylene blue dye.

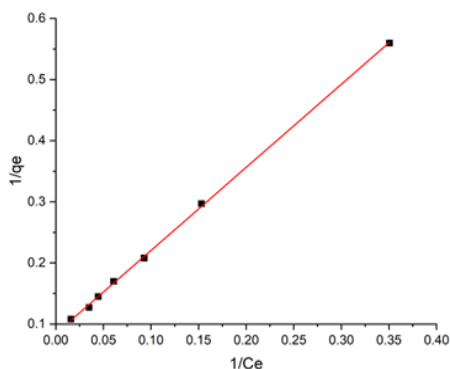


Fig. 11. Langmuir modelling plot for adsorption

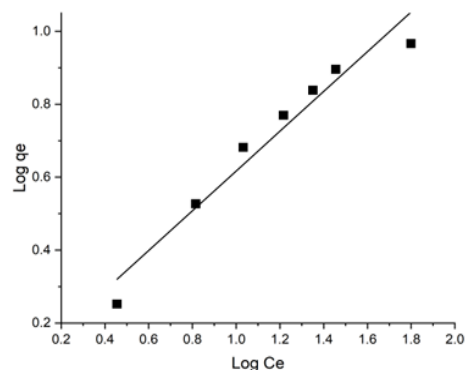


Fig. 12. Freundlich modelling plot for of MB onto ACCAL

Table 6. Adsorption Isotherm plots parameters for MB adsorption onto ACCAL_{KHCO₃}

Langmuir - ACCAL _{KHCO₃}				Freundlich -ACCAL _{KHCO₃}		
R ²	Q _{max} (mg/g)	K _L (L/mg)	R _L	R ²	K _F (mg/g)	1/n
0.999	11.83	0.062	0.6163	0.9519	3.506	0.5117

Table 7. Comparison of adsorption capacity of activated carbons (Adsorbent)

Adsorbents	Maximum Adsorption Capacity (Q _m) (mg/g)	References
Rice husks	9.8	Sharma et al., [66]
Fig leaves	41.7	Al-Asadi et al. [67]
Orange peel	18.6	Annadurai et al., [68]
Cola nut shells	87.12	Ndi et al., [69]
Coconut shells	15.2	Khuluk et al., [50]
Bush cane bark powder	23.49	Enenebeaku et al., [28]
Rice husks	26.3	Sawasdee et al., [53]
Costus afer leaves	11.83	This work

3.6 Comparative Analysis of Other Adsorbents

The comparison of a few adsorbents, including CAL, and their maximum MB adsorption capacity is shown in Table 7. This initial investigation into ACCAL's adsorption capacity shows that it has great potential for eliminating coloring materials from aqueous solutions. The material's significant cost reduction and ease of accessibility outweigh its adsorption capabilities, which are somewhat lower than those of many other known adsorbents. These early results call for more research, including the use of acids or bases to activate the adsorbent (CAL), higher impregnation ratio, isotherm studies, and continuous flow operations to assess the adsorption capabilities of ACCAL.

4. CONCLUSION

This work underscores the potential of Costus afer leaves (CAL) waste as a cost-effective, sustainable, and eco-friendly adsorbent for the removal of methylene blue dye from aqueous solutions. The proximate analysis of CAL precursors revealed favorable characteristics, such as high fixed carbon content and low ash content, indicating their suitability for activated carbon production. Characterization of the activated carbon using Fourier transform infrared spectroscopy (FTIR), Scanning electron microscopy (SEM), and Energy dispersive X-ray (EDX) corroborated previous research and provided a comprehensive understanding of the material's structure and composition. Batch studies demonstrated that the adsorption of methylene blue was influenced by parameters

such as dosage, contact time, and pH. Optimal conditions for maximum adsorption efficiency were determined to be an adsorbent dose of 0.2g, contact time of 10 minutes, and pH of 8. Under these conditions, activated Costus afer leaves (KHCO_3) achieved a remarkable percentage removal rate of 70.58% with a maximum adsorption capacity of 11.83 mg/g for $\text{ACCAL}_{\text{KHCO}_3}$. These findings highlight the potential of Costus afer leaves as a promising adsorbent for water treatment applications. Further research could explore scaling up the production of activated carbon from CAL and investigating its performance with increasing impregnation ratio, and temperature. Overall, this work contributes to the growing body of knowledge on sustainable solutions for wastewater remediation.

COMPETING INTERESTS

Authors have declared that no competing interests exist.

REFERENCES

- Okafor CC. SHELL Center for Environmental Management and Control, University of Nigeria, Enugu Campus, Enugu 410001, Nigeria, Madu CN, Ajaero CC, Ibekwe JC, Nzekwe CA. Department of Management and Management Science, Lubin School of Business, Pace University, New York, NY 10038, USA. Sustainable management of textile and clothing. *Clean Technologies and Recycling*. 2021;1(1):70–87. DOI:10.3934/ctr.2021004
- Demirbas A. Agricultural based activated carbons for the removal of dyes from aqueous solutions: A review. *Journal of Hazardous Materials*. 2009;167(1–3):1–9. DOI:10.1016/j.jhazmat.2008.12.114
- Senthilkumaar S, Varadarajan PR, Porkodi K, Subbhuraam CV. Adsorption of methylene blue onto jute fiber carbon: Kinetics and equilibrium studies. *Journal of Colloid and Interface Science*. 2005;284(1):78–82.
- Ahmed MJ, Theydan SK. Equilibrium isotherms, kinetics and thermodynamics studies of phenolic compounds adsorption on palm-tree fruit stones. *Ecotoxicology and Environmental Safety*. 2012;84:39–45. DOI:10.1016/j.ecoenv.2012.06.019
- Chowdury SBA, Hamid R, Das MR, Hasan SM, Zain K, Khalid MD. Uddin. *Journal of Bioresources*. 2013;8(4):6523–6555.
- Ali I. New Generation Adsorbents for Water Treatment. *Chemical Reviews*. 2012;112:5073–5091.
- Liu Y, Zheng Y, Wang A. Enhanced adsorption of Methylene Blue from aqueous solution by chitosan-g-poly (acrylic acid) vermiculite hydrogel composites. *Journal of Environmental Sciences (China)*. 2010;22(4):486–493. DOI: 10.1016/s1001-0742(09)60134-0
- Khan MA, Uddin MK, Bushra R, Ahmad A, Nabi SA. Synthesis and characterization of polyaniline Zr(IV) molybdophosphate for the adsorption of phenol from aqueous solution. *Reaction Kinetics Mechanisms and Catalysis*. 2014;113(2):499–517. DOI: 10.1007/s11144-014-0751-x
- Faouzi Elahmadi M, Bensalah N, Gadri A. Treatment of aqueous wastes contaminated with Congo Red dye by electrochemical oxidation and ozonation processes. *Journal of Hazardous Materials*. 2009;168(2–3):1163–1169. DOI: 10.1016/j.jhazmat.2009.02.139
- Crini G. Non-conventional low-cost adsorbents for dye removal: A review. *Bioresource Technology*. 2006;97(9):1061–1085. DOI: 10.1016/j.biortech.2005.05.001
- Garg VK, Gupta R, Bala Yadav A, Kumar R. Dye removal from aqueous solution by adsorption on treated sawdust. *Bioresource Technology*. 2003;89(2):121–124. DOI: 10.1016/s0960-8524(03)00058-0
- Janos P, Buchtová H, Rýznarová M. Sorption of dyes from aqueous solutions onto fly ash. *Water Research*. 2003;37(20):4938–4944. DOI: 10.1016/j.watres.2003.08.011
- Singh H, Chauhan G, Jain AK, Sharma SK. Adsorptive potential of agricultural wastes for removal of dyes from aqueous solutions. *Journal of Environmental Chemical Engineering*. 2017;5(1):122–135. DOI: 10.1016/j.jece.2016.11.030
- Elsagh A, Moradi O, Fakhri A, Najafi F, Alizadeh R, Haddadi V. Evaluation of the potential cationic dye removal using adsorption by graphene and carbon nanotubes as adsorbents surfaces. *Arabian Journal of Chemistry*. 2017;10:S2862–S2869. DOI: 10.1016/j.arabjc.2013.11.013

15. Gupta VK, Kumar R, Nayak A, Saleh TA, Barakat MA. Adsorptive removal of dyes from aqueous solution onto carbon nanotubes: A review. *Advances in Colloid and Interface Science*. 2013;193–194:24–34.
DOI: 10.1016/j.cis.2013.03.003
16. Benedetti V, Patuzzi F, Baratieri M. Characterization of char from biomass gasification and its similarities with activated carbon in adsorption applications. *Applied Energy*. 2018;227:92–99.
Available:https://doi:10.1016/j.apenergy.2017.08.076
17. Ganjoo R, Sharma S, Kumar A, Daouda MMA. Activated carbon: Fundamentals, classification, and properties. In *Activated Carbon*. 2023;1–22.
DOI: 10.1039/bk9781839169861-00001
18. Yiling J. Preparation of activated carbon from walnut shell and its application in industrial wastewater. *AIP conference proceedings*. 2017;1839:020063.
Available:https://doi.org/10.1063/1.4982428
19. Fan C, Li Y, Liu X, Chen S, Yuan S. Preparation of activated carbon from peanut shells by KOH activation for methylene blue and lead ions adsorption. *Journal of Environmental Chemical Engineering*. 2017;5(1):29-36.
Available:https://doi:10.1016/j.jece.2016.11.022
20. Asadu CO, Anthony EC, Elijah OC, Ike IS, Onoghwarite OE, Okwudili UE. Development of an adsorbent for the remediation of crude oil polluted water using stearic acid grafted coconut husk (*Cocos nucifera*) composite. *Applied Surface Science Advances*. 2021; 6(100179):100179.
DOI: 10.1016/j.apsadv.2021.100179
21. Alongamo BAA, Ajifack LD, Ghogomu JN, Nsami NJ, Ketcha JM. Activated carbon from the peelings of cassava tubers (*Manihot esculenta*) for the removal of nickel (II) ions from aqueous solution. *Journal of Chemistry*, 2021;1–14.
DOI: 10.1155/2021/5545110
22. Gumus RH, Okpeku I. Production of activated carbon and characterization from snail shell waste (*Helix pomatia*). *Advances in Chemical Engineering and Science*. 2015;05(01):51–61.
DOI: 10.4236/aces.2015.51006
23. Ekpete OA, Marcus AC, Osi V. Preparation and Characterization of Activated Carbon Obtained from Plantain (*Musa paradisiaca*) Fruit Stem. *Journal of Chemistry*; 2017.
Available:https://doi.org/10.1155/2017/8635615
24. Menendez-Diaz JA, Martin-Gullon I. Types of Carbon Adsorbents and Their Production, in *Activated Carbon Surfaces in Environmental Remediation*, edited by Bandosz TJ. Academic Press, New York. 2006;1-47.
25. Khodaie M, Ghasemi N, Moradi B, Rahimi M. Removal of methylene blue from wastewater by adsorption onto ZnCl₂ Activated corn husk carbon equilibrium studies. *Journal of Chemistry*. 2013;1–6.
DOI: 10.1155/2013/383985
26. Castalino M, Aravinda HB. Methylene blue dye removal from aqueous solution by utilization of groundnut shell activated carbon. *International Research Journal of Engineering and Technology*. 2020;7: 2495-2499.
27. Baloo L, Isa MH, Sapari NB, Jagaba AH, Wei LJ, Yavari S, Vasu R. Adsorptive removal of methylene blue and acid orange 10 dyes from aqueous solutions using oil palm wastes-derived activated carbons. *Alexandria Engineering Journal*. 2021;60(6):5611–5629.
DOI: 10.1016/j.aej.2021.04.044
28. Enenebeaku CK, Okorochoa NJ, Enenebeaku UE, Onyeachu BI. Adsorption of methylene blue dye onto bush cane bark powder. *International Letters of Chemistry Physics and Astronomy*. 2017;76:12–26.
DOI:10.18052/www.scipress.com/ilcpa.76.12
29. Boison D, Adinortey CA, Babanyinah GK, Quasie O, Agbeko R, Wiabo-Asabil GK, Adinortey MB. *Costus afer*: A systematic review of evidence-based data in support of its medicinal relevance. *Scientifica*. 2019;3732687
DOI: 10.1155/2019/3732687
30. ThankGod NK, Monago C, Anacletus F. Antihyperglycemic activity of the aqueous extract of *Costus afer* stem alone and in combination with metformin. *European Journal of Biotechnology and Bioscience*; 2014.
Available:https://www.semanticscholar.org/paper/38a13cc15463713dc4ac91f6e0b3a57c209

31. Anyasor G, Onajobi F, Osilesi O, Adebawo O. Hexane fraction of *Costus afer* Ker Gawl leaf inhibited mitochondrial permeability transition, F1F0 ATPase and scavenged nitric oxide and hydrogen peroxide (957.1). *FASEB Journal: Official Publication of the Federation of American Societies for Experimental Biology*. 2014; 28(S1).
DOI:10.1096/fasebj.28.1_supplement.957.1
32. Udem SC, Ezeasor CK. The acute and subchronic toxicity studies of aqueous leaf and stem bark extract of *Costus afer* ker (*Zingiberaceae*) in mice. *Comparative Clinical Pathology*. 2010; 19(1):75–80.
DOI: 10.1007/s00580-009-0906-8
33. Liu C, Li F, Ma LP, Cheng HM. Advanced materials for energy storage. *Advanced Materials (Deerfield Beach, Fla.)*. 2010; 22(8):E28-62.
DOI: 10.1002/adma.200903328
34. Ali I, Asim M, Khan TA. Low cost adsorbents for the removal of organic pollutants from wastewater. *Journal of Environmental Management*. 2012;113: 170–183.
DOI:10.1016/j.jenvman.2012.08.028 (Raw preparation)
35. Fito J, Said H, Feleke S, Worku A. Fluoride removal from aqueous solution onto activated carbon of *Catha edulis* through the adsorption treatment technology. *Environmental Systems Research*. 2019; 8(1).
DOI: 10.1186/s40068-019-0153-1
36. Moges A, Nkambule TTI, Fito J. The application of GO-Fe₃O₄ nanocomposite for chromium adsorption from tannery industry wastewater. *Journal of Environmental Management*. 2022; 305(114369):114369.
DOI: 10.1016/j.jenvman.2021.114369
37. Fito J, Abewaa M, Nkambule T. Magnetite-impregnated biochar of parthenium hysterophorus for adsorption of Cr(VI) from tannery industrial wastewater. *Appl Water Sci*. 2023;13:78.
Available:https://doi.org/10.1007/s13201-023-01880-y
38. Stabentheiner E, Zankel A, Pölt P. Environmental scanning electron microscopy (ESEM)--a versatile tool in studying plants. *Protoplasma*. 2010;246(1–4):89–99.
DOI: 10.1007/s00709-010-0155-3
39. Bedmohata MA, Chaudhari AR, Singh SP, Choudhary MD. Adsorption capacity of activated carbon prepared by chemical activation of lignin for the removal of methylene blue dye. *International Journal of Advanced Research in Chemical Science*. 2015;2(8):1-13.
40. Asadu CO, Elijah OC, Ogbodo NO, Anthony EC, Onyejiuwa CT, Onoh MI, Chukwuebuka AS. Treatment of crude oil polluted water using stearic acid grafted mango seed shell (*Mangifera indica*) composite. *Current Research in Green and Sustainable Chemistry*. 2021;4(100169): 100169.
DOI: 10.1016/j.crgsc.2021.100169
41. Obayomi KS, Lau SY, Zahir A, Meunier L, Zhang J, Dada AO, Rahman MM. Removing methylene blue from water: A study of sorption effectiveness onto nanoparticles-doped activated carbon. *Chemosphere*. 2023;313(137533):137533.
DOI: 10.1016/j.chemosphere.2022.137533
42. Guan F, Tao J, Yao Q, Li Z, Zhang Y, Feng S, et al. Alginate-based aerogel fibers with a sheath-core structure for highly efficient methylene blue adsorption via directed freezing wet-spinning. *Colloids Surfaces A Physicochem. Eng. Aspects*. 2024;680:132706.
DOI: 10.1016/j.colsurfa.2023.132706
43. Russo AV, Merlo BG, Jacobo SE. Adsorption and catalytic degradation of Tartrazine in aqueous medium by a Fe-modified zeolite. *Cleaner Engineering and Technology*. 2021;4(100211):100211.
DOI: 10.1016/j.clet.2021.100211
44. Dehghani MH, Gholami S, Karri RR, Lima EC, Mahvi AH, Nazmara S, Fazlzadeh M. Process modeling, characterization, optimization, and mechanisms of fluoride adsorption using magnetic agro-based adsorbent. *Journal of Environmental Management*. 2021;286(112173):112173.
DOI: 10.1016/j.jenvman.2021.112173
45. Langmuir I. The adsorption of gases on plane surfaces of glass, mica and platinum. *Journal of the American Chemical Society*. 1918;40(9):1361–1403.
DOI: 10.1021/ja02242a004
46. Almasi A, Rostamkhani Z, Mousavi SA. Adsorption of Reactive Red 2 using activated carbon prepared from walnut shell: Batch and fixed bed studies. *Desalination and Water Treatment*. 2017;79:356–367.
DOI: 10.5004/dwt.2017.20791

47. Freundlich HM. Over the adsorption in solution. The Journal of Physical Chemistry A. 1906;57:385-470. Available:https://doi.org/10.1515/zpch-1907-5723
48. Fazal A, Rafique U. Severance of lead by acetylated and esterified spent camellia sinensis Powder, Am. J. Environ. Eng. 2013;3(6):288–296. Available:http://dx.doi.org/10.5923/j.ajee.20130306.04
49. Fito J, Abewaa M, Mengistu A, Angassa K, Ambaye AD, Moyo W, Nkambule T. Adsorption of methylene blue from textile industrial wastewater using activated carbon developed from Rumex abyssinicus plant. Scientific Reports. 2023;13(1): 5427. DOI: 10.1038/s41598-023-32341-w
50. Khuluk RH, Rahmat A, Buhani B, Suharso S. Removal of methylene blue by adsorption onto activated carbon from coconut shell (*Cocous nucifera L.*). Indonesian Journal of Science and Technology. 2019;4(2):229–240. DOI:10.17509/ijost.v4i2.18179
51. Dimbo D, Abewaa M, Adino E, Mengistu A, Takele T, Oro A, Rangaraju M. Methylene blue adsorption from aqueous solution using activated carbon of *Spathodea campanulata*. Results in Engineering. 2024;21(101910):101910. DOI: 10.1016/j.rineng.2024.101910
52. Kumari G, Soni B, Karmee SK. Synthesis of activated carbon from groundnut shell via chemical activation. Journal of the Institution of Engineers (India) Series E. 2022;103(1):15–22. DOI: 10.1007/s40034-020-00176-z
53. Sawasdee S. Faculty of Science and Technology, Thepsatri Rajabhat University, Lop Buri 15000, Thailand, Watcharabundit P, and Faculty of Science and Technology, Thepsatri Rajabhat University, Lop Buri 15000, Thailand. Characterization and adsorption mechanism of methylene blue dye by mesoporous activated carbon prepared from rice husks. Environment and Natural Resources Journal. 2023; 21(5):1–13. DOI: 10.32526/enrj/21/20230074
54. Lazzarini A, Piovano A, Pellegrini R, Agostini G, Rudić S, Lamberti C, Groppo E. Graphitization of activated carbons: A molecular-level investigation by INS, DRIFT, XRD and Raman techniques. Physics Procedia. 2016;85:20–26. DOI: 10.1016/j.phpro.2016.11.076
55. Hidayu AR, Muda N. Preparation and characterization of impregnated activated carbon from palm kernel shell and coconut shell for CO₂ capture. Procedia Engineering. 2016;148:106–113. DOI: 10.1016/j.proeng.2016.06.463
56. Nasir S, Hussein M, Zainal Z, Yusof N, Mohd Zobir S. Electrochemical energy storage potentials of waste biomass: Oil palm leaf- and palm kernel shell-derived activated carbons. Energies. 2018;11(12): 3410. DOI: 10.3390/en11123410
57. Maulina S, Mentari VA. Comparison of functional group and morphological surface of activated carbon from oil palm fronds using phosphoric acid (H₃PO₄) and nitric acid (HNO₃) as an activator. IOP Conference Series. Materials Science and Engineering. 2019;505(1): 012023. DOI: 10.1088/1757-899x/505/1/012023
58. Nuru S, Angassa K, Tibebe S, Kebede S, Mulu A. Adsorption of chemical oxygen demand from surface water using bagasse activated carbon. Sustainable Water Resources Management. 2023;9(6). DOI: 10.1007/s40899-023-00961-9
59. Dahri MK, Kooh MRR, Lim LBL. Application of Casuarina equisetifolia needle for the removal of methylene blue and malachite green dyes from aqueous solution. Alexandria Engineering Journal. 2015;54(4):1253–1263. DOI: 10.1016/j.aej.2015.07.005
60. Geçgel Ü, Özcan G, Gürpınar GÇ. Removal of methylene blue from aqueous solution by activated carbon prepared from pea shells (*Pisum sativum*). Journal of Chemistry. 2013;1–9. DOI: 10.1155/2013/614083
61. Peng W, Li H, Liu Y, Song S. Adsorption of methylene blue on graphene oxide prepared from amorphous graphite: Effects of pH and foreign ions. Journal of Molecular Liquids. 2016;221:82–87. DOI: 10.1016/j.molliq.2016.05.074
62. Felista MM, Wanyonyi WC, Ongera G. Adsorption of anionic dye (Reactive black 5) using macadamia seed Husks: Kinetics and equilibrium studies. Scientific African. 2020;7(e00283):e00283. DOI: 10.1016/j.sciaf.2020.e00283
63. Teweldebrihan MD, Gnaro MA, Dinka MO. The application of magnetite biochar

- composite derived from parthenium hysterophorus for the adsorption of methylene blue from aqueous solution. *Frontiers in Environmental Science*. 2024;12.
DOI: 10.3389/fenvs.2024.1375437
64. Malik PK. Dye removal from wastewater using activated carbon developed from sawdust: Adsorption equilibrium and kinetics. *Journal of Hazardous Materials*. 2004;113(1–3):81–88.
DOI: 10.1016/j.jhazmat.2004.05.022
65. Arora C, et al. Iron based metal organic framework for efficient removal of methylene blue dye from industrial waste. *J. Mol. Liq.* 2019;284:343–352 (Adsorption)
66. Sharma YC, Uma. Optimization of parameters for adsorption of methylene blue on a low-cost activated carbon. *Journal of Chemical and Engineering Data*. 2010;55(1):435–439.
DOI: 10.1021/je900408s
67. Al-Asadi ST, Al-Qaim FF. Adsorption of Methylene Blue Dye from aqueous solution using low cost adsorbent: Kinetic, Isotherm Adsorption and Thermodynamic Studies; 2023.
DOI: 10.21203/rs.3.rs-2449414/v1
68. Annadurai G, Juang RS, Lee DJ. Use of cellulose-based wastes for adsorption of dyes from aqueous solutions. *Journal of Hazardous Materials*. 2002;92(3):263–274.
DOI: 10.1016/s0304-3894(02)00017-1
69. Ndi Nsami J, Ketcha Mbadcam J. The adsorption efficiency of chemically prepared activated carbon from cola nut shells by on methylene blue. *Journal of Chemistry*. 2013;1–7.
DOI: 10.1155/2013/469170

© Copyright (2024): Author(s). The licensee is the journal publisher. This is an Open Access article distributed under the terms of the Creative Commons Attribution License (<http://creativecommons.org/licenses/by/4.0>), which permits unrestricted use, distribution, and reproduction in any medium, provided the original work is properly cited.

Peer-review history:
The peer review history for this paper can be accessed here:
<https://prh.ikprress.org/review-history/12060>